Robotica (2012) volume 30, pp. 467–475. © Cambridge University Press 2011
doi:10.1017/S026357471100083X

A novel three degrees of freedom partially decoupled robot with linear actuators

Jaime Gallardo-Alvarado†,*, Gürsel Alici‡ and Ramón Rodríguez-Castro†

†*Department of Mechanical Engineering, Instituto Tecnológico de Celaya, Av. Tecnológico y A. García Cubas, 38010 Celaya, GTO, México*
‡*School of Mechanical, Materials, and Mechatronic Engineering, University of Wollongong, 2522 NSW, Australia*

(Received in Final Form: June 21, 2011; accepted June 22, 2011. First published online: July 21, 2011)

SUMMARY
In this work, a new translational robot formed with two different parallel manipulators with a common control point is introduced. An asymmetric parallel manipulator provides three translational degrees of freedom to the proposed robot while the orientation of the end-effector platform is kept constant by means of a Delta-like manipulator. An exact solution is easily derived to solve the forward displacement analysis while a semi-closed form solution is available for solving the inverse displacement analysis. The infinitesimal kinematics of the robot is approached by applying the theory of screws. Finally, a numerical example that consists of solving the inverse/forward displacement analysis as well as the forward acceleration analysis of the end-effector platform is presented. The example also includes the computation of the workspace and the direct/inverse singularities of the example.

KEYWORDS: Design; Parallel manipulators; Space robotics; Novel applications of robotics; Decoupled.

1. Introduction

Parallel manipulators with fewer than six degree of freedom have a wide range of applications, including assembly, machining, micro robotics, and medical applications. Therefore, in spite of a limited mobility, they have gained an increasing interest in research as well as in industry. Fruitful results have been obtained in this trend, for details visit the website.[1]

Without doubt nowadays, the most celebrated parallel manipulator with fewer than six degrees of freedom is the robot Delta invented by Clavel,[2] a translational parallel manipulator (TPM) designed for pick-and-place operations. Before the success of the robot Delta, TPMs become one of the most attractive class of lower mobility parallel manipulators, Table I listed some contributions in this research field.

The TPMs listed in Table I exhibit a common characteristic: identical limbs and therefore frequently these are denominated as symmetric parallel manipulators. If the forward displacement analysis (FDA), a challenging task of most parallel manipulators of a TPM can be carried-out by solving a set of linear equations then the parallel manipulator is known as a three degree of freedom linear TPM.[16,17] In that way, the contribution of Kong and Gosselin[7] concerning with the kinematic and singularity analyses of the 3-CRR TPM is one of the most known efforts devoted to simplify the forward kinematics of a TPM. As it is pointed by one of the reviewers, the 3-CRR robot was previously investigated in Carricato and Parenti-Castelli.[18] Furthermore, it is said that a TPM is fully decoupled if each one of its degrees of freedom is affected by one, and only one, generalized coordinate, perhaps a perfect mechanism from a kinematic point of view. As it is shown in Carricato and Parenti-Castelli,[18] the merits of a fully decoupled TPM allows to obtain fully isotropic mechanisms free of singularities. Recently, Briot and Bonev[19] proposed a fully decoupled isotropic translational parallel mechanism, named the Pantopteron, constructed with three pantograph linkages. However, this robot is recommended only for pick-and-place operations.

In this work a new TPM with uncoupled kinematics is introduced. The proposed robot consists of two parallel manipulators that share a control point attached at their moving platforms. The position of the control point is conducted by means of an asymmetric parallel manipulator while the constant orientation of the end-effector-platform is achieved by means of a Delta-like manipulator. The theory of screws is the mathematical resource to approach the velocity and acceleration analyses. Simple and compact expressions for solving the infinitesimal kinematics of the proposed robot are carried out by taking advantage of the concept of reciprocal screws.

2. Description of the Translational Robot

The proposed robot, see Fig. 1, consists of an external parallel manipulator (EPM) and an inner parallel manipulator (IPM). Both spatial mechanisms share a spherical joint over their moving platforms whose centroid is chosen as the control point C_m of the robot.

The IPM is a TPM[20] whose role is to keep constant the orientation of the end-effector platform with respect to the fixed platform, whereas the EPM is a three-legged

* Corresponding author. E-mail: gjaime@itc.mx

https://doi.org/10.1017/S026357471100083X Published online by Cambridge University Press

Table I. Some TPMs.

Author(s)	Proposed or investigated architecture
L.-W. Tsai[3]	3-UPU
P. Wenger and D. Chablat[4]	The Orthoglide
T. S. Zhao and Z. Huang[5]	3-RRC
R. Di Gregorio[6]	3-URC
X. Kong and C. M Gosselin[7]	3-CRR
M. Callegari and M. Tarantini[8]	3-RPC
G. Gogu[9,10]	Isoglide
Y. Li and X. Xu[11]	3-PRC
W. Li, F. Gao and J. Zhang[12]	R-CUBE
M. Callegari, M, Palpacelli and Marco Scarponi[13]	3-CPU
M. Callegari, M.-C. Palpacelli and M. Principi[14]	3-RCC
M. Ruggiu[15]	3-CUR

C = cylindrical joint, P = prismatic joint, R = revolute joint, S = spherical joint, U = universal joint.

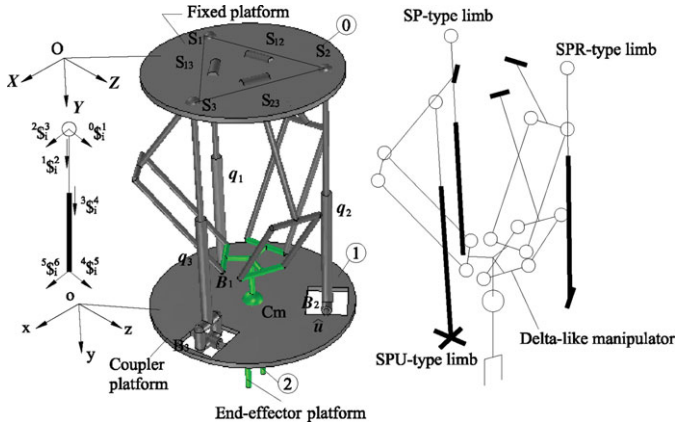

Fig. 1. (Colour online) The proposed robot and its geometric scheme.

asymmetric parallel manipulator, SP + SPR + SPU, whose function is to provide three translational movements to the control point and it is an adaptation of the four degrees of freedom partially decoupled parallel manipulator introduced by Gallardo-Alvarado *et al.*[21] The adjustable-length limbs $q_i (i = 1, 2, 3)$, with associated vectors $\boldsymbol{q}_i$(in the remainder of this work $i = 1, 2, 3$), are chosen as the active kinematic pairs of the robot and since they provide rectilinear forces, then the proposed manipulator can be used not only as a pick-and-place manipulator but also as a spatial translational machine tool.

The robot features three spherical joints with centers $S_i = (X_i, Y_i, Z_i)$, which form an equilateral triangle $\Delta S_1 S_2 S_3$ with side e, which are located by vectors $\boldsymbol{S}_i$, and three revolute joints with a tangential arrangement in the fixed platform. The points B_1, B_2, and B_3 located by vectors $\boldsymbol{B}_i$ denote the nominal positions of the fixed, revolute, and universal joints in the coupler platform of the IPM. The axis of the revolute joint of the SPR limb is parallel to the line B_1B_3 whereas the axis of the revolute joint connecting the SPU limb to the coupler platform, representing one freedom of the universal joint, is parallel to the line B_1B_2. Finally, the SP limb is normal to the plane $\Delta B_1 B_2 B_3$.

3. Finite Kinematics

In this section, the forward and inverse displacement analyses are carried out by using simple geometric procedures. The FDA consists of finding the position of the control point Cm given a set of generalized coordinates or active length limbs q_i whereas the inverse displacement analysis (IDA) consists of finding the active length limbs of the robot given the instantaneous coordinates of the control point Cm.

3.1. Forward displacement analysis

Let O_XYZ be a global reference frame attached at the fixed platform with the origin O placed at the center of the equilateral triangle $\Delta S_1 S_2 S_3$ and the Y-axis normal to the plane of such triangle. Similarly, let o_xyz be a moving reference frame attached at the coupler platform with the origin o placed at the center of the equilateral triangle $\Delta B_1 B_2 B_3$ and the y-axis normal to the plane of such triangle. In order to simplify the FDA, in what follows, as an intermediate step, the position vector of point O with respect to point o, vector $\boldsymbol{r}_{O/o}$, expressed in the reference frame o_{xyz} will be computed. To this end, with reference to Fig. 1(a), simple loop-closure equation is readily written as

$$\boldsymbol{S}_1 = \boldsymbol{B}_1 + \boldsymbol{q}_1, \tag{1}$$

where $\boldsymbol{q}_1$ is a vector along the y-axis. Moreover, the revolute joint, with associated unit vector $\hat{\boldsymbol{u}}$ along the corresponding axis, of the SPR limb constraints the vector $\boldsymbol{S}_2 - \boldsymbol{B}_2$ in such a way that

$$(\boldsymbol{S}_2 - \boldsymbol{B}_2) \bullet \hat{\boldsymbol{u}} = 0, \tag{2}$$

where the bullet $\bullet$ denotes the usual inner product of three-dimensional vectorial algebra. Furthermore, from the triangle $\Delta S_1 S_2 B_2$, two compatibility equations are given by

$$\left.\begin{aligned}(\boldsymbol{S}_2 - \boldsymbol{S}_1) \bullet (\boldsymbol{S}_2 - \boldsymbol{S}_1) - e^2 = 0,\\ (\boldsymbol{S}_2 - \boldsymbol{B}_2) \bullet (\boldsymbol{S}_2 - \boldsymbol{B}_2) - q_2^2 = 0.\end{aligned}\right\} \tag{3}$$

After a few computation, Eqs. (1)–(3) yield a second-order algebraic equation in the unknown Y_2 as

$$K_3 Y_2^2 + K_4 Y_2 + K_5 = 0, \tag{4}$$

whereas the remaining coordinates of S_2 are obtained upon linear equations as

$$X_2 = K_1 Y_2 + K_2, \quad Z_2 = K_6 Y_2 + K_7, \tag{5}$$

where the coefficients $K_j (j = 1, 2, \ldots, 7)$, which are provided in Appendix, are calculated according to the given coordinates of the points S_1, B_1, B_2 and the length limb q_2.

https://doi.org/10.1017/S026357471100083X Published online by Cambridge University Press

Following a similar procedure and considering the closure equations given by

$$\left.\begin{aligned}(\boldsymbol{S}_3-\boldsymbol{S}_1)\bullet(\boldsymbol{S}_3-\boldsymbol{S}_1)-e^2=0,\\(\boldsymbol{S}_3-\boldsymbol{S}_2)\bullet(\boldsymbol{S}_3-\boldsymbol{S}_2)-e^2=0,\\(\boldsymbol{S}_3-\boldsymbol{B}_3)\bullet(\boldsymbol{S}_3-\boldsymbol{B}_3)-q_3^2=0.\end{aligned}\right\} \tag{6}$$

A second-order algebraic equation in the unknown Y_3 results in

$$K_{10}Y_3^2+K_{11}Y_3+K_{12}=0, \tag{7}$$

while the remaining coordinates of point S_3 are obtained as

$$X_3=K_8Y_3+K_9, \quad Z_3=K_{13}Y_3+K_{14}, \tag{8}$$

where the coefficients $K_j(j=8,9,\ldots,14)$ depend on the coordinates of the points S_1, S_2, B_3 and the length limb q_3 and are given in Appendix.

Once the coordinates of points S_i are calculated, the position vector $\boldsymbol{r}_{O/o}$, denoting the relative position of the origins of the reference frames, is computed as

$$\boldsymbol{r}_{O/o}=(\boldsymbol{S}_1+\boldsymbol{S}_2+\boldsymbol{S}_3)/3. \tag{9}$$

Furthermore, the 4×4 homogeneous transformation matrix of the fixed platform, with respect to the coupler platform, is given by

$${}^1\mathbf{T}^0=\begin{bmatrix}{}^1\mathbf{R}^0 & \boldsymbol{r}_{O/o}\\ 0_{1\times3} & 1\end{bmatrix}, \tag{10}$$

where ${}^1\mathbf{R}^0$ is the rotation matrix of the fixed platform with respect to the coupler platform, which can be computed using the method introduced in Gallardo-Alvarado *et al.*[22] Finally, taking into account that

$${}^0\mathbf{T}^1\ {}^1\mathbf{T}^0=\mathbf{I}_4, \tag{11}$$

where $\mathbf{I}_4$ is the identity matrix of dimension 4, then the homogeneous transformation matrix of the coupler platform with respect to the fixed platform is obtained as the inverse of ${}^1\mathbf{T}^0$. Furthermore, the coordinates of any point P, including the control point Cm attached at the coupler platform, expressed in the global reference frame O_XYZ, can be obtained by means of the relationship

$$\begin{bmatrix}P\\1\end{bmatrix}={}^0\mathbf{T}^1\begin{bmatrix}p\\1\end{bmatrix}, \tag{12}$$

where p is expressed in the moving reference frame o_xyz.

Finally, according to Eqs. (4) and (7), points S_2 and S_3 can reach, each one, at most two positions. Hence, there are at most four feasible poses of the end-effector platform with respect to the fixed platform for a prescribed set of generalized coordinates q_i. Moreover, the actual configuration of the manipulator can be easily determined due to the fact that the user is free to select the sign for each discriminant associated to Eqs. (4) and (7). Furthermore, it should be noted that one freedom between the coupler and fixed platforms is affected only by the generalized coordinate q_1 while the remaining two degrees of freedom are affected simultaneously by q_2 and q_3; in that way, it is possible to affirm that the proposed TPM possesses partially decoupled degrees of freedom.

3.2. Inverse displacement analysis

From the equilateral triangle $\Delta B_1B_2B_3$ in Fig. 1, one obtains

$$(\boldsymbol{B}_1+\boldsymbol{B}_2+\boldsymbol{B}_2)/3=\boldsymbol{C}_m, \tag{13}$$

whereas according to the tangential arrangement of the revolute joint B_2 it is possible to write

$$(\boldsymbol{B}_2-\boldsymbol{S}_2)\bullet(\boldsymbol{B}_3-\boldsymbol{B}_1)=0. \tag{14}$$

On the other hand, the SP-type limb restricts the motions of the coupler platform in such a way that

$$(\boldsymbol{B}_1-\boldsymbol{S}_1)\bullet(\boldsymbol{B}_2-\boldsymbol{B}_1)=0, \tag{15}$$

and

$$(\boldsymbol{B}_1-\boldsymbol{S}_1)\bullet(\boldsymbol{B}_3-\boldsymbol{B}_1)=0. \tag{16}$$

Finally, three compatibility kinematic constraints are given by

$$(\boldsymbol{B}_i-\boldsymbol{B}_j)\bullet(\boldsymbol{B}_i-\boldsymbol{B}_j)-B_{ij}^2=0 \quad i,j=1,2,3 \mod(3), \tag{17}$$

where B_{ij} is the distance between points B_i and B_j.

Expressions (13)–(17) represent a system of nine equations in nine unknowns that can be solved by means of continuation methods, for details the reader is referred to Tsai.[23] Finally, the length limbs are computed as follows:

$$q_i^2=(\boldsymbol{B}_i-\boldsymbol{S}_i)\bullet(\boldsymbol{B}_i-\boldsymbol{S}_i). \tag{18}$$

4. Infinitesimal Kinematics

This section addresses the inverse/forward velocity and acceleration analyses of the proposed robot by means of the theory of screws. The modeling of the screws is depicted in Fig. 1. Each spherical joint of the EPM is simulated by means of three revolute joints with associated screws ${}^0\$_i^1$, ${}^1\$_i^2$, and ${}^2\$_i^3$ whose primal parts, or directions, intersect at the center S_i of the corresponding spherical joint and the direction of the screw ${}^1\$_i^2$ is along the S_iB_i line. Whereas the screw ${}^3\$_i^4$ is associated to the ith prismatic joint and therefore its pitch goes to infinity. On the other hand, the connection of the limbs to the coupler platform is simulated, each one, by means of two revolute joints, sometimes virtual elements, represented by screws ${}^4\$_i^5$ and ${}^5\$_i^6$ whose primal parts intersect at the corresponding point B_i. Naturally, the pitch of every screw representing a revolute joint is equal to zero.

https://doi.org/10.1017/S026357471100083X Published online by Cambridge University Press

4.1. Velocity analysis

The velocity state of the coupler platform with respect to the fixed platform taking the origin of the global reference frame as the reference pole, $\boldsymbol{V}_O = [\mathcal{P}(\boldsymbol{V}_O) = \boldsymbol{\omega}, \mathcal{D}(\boldsymbol{V}_O) = \boldsymbol{v}_O]^{\mathrm{T}}$, can be written through any of the limbs of the EPM as follows:

$$\mathbf{J}_i \Omega_i = \boldsymbol{V}_O, \tag{19}$$

where $\mathbf{J}_i = [{}^0\$_i^1, {}^1\$_i^2, {}^2\$_i^3, {}^3\$_i^4, {}^4\$_i^5, {}^5\$_i^6]$ is the Jacobian of the ith limb, $\Omega_i = [{}_0\omega_1^i, {}_1\omega_2^i, {}_2\omega_3^i, {}_3\omega_4^i, {}_4\omega_5^i, {}_5\omega_6^i]^{\mathrm{T}}$ is matrix containing the joint velocity rates of the ith limb. It is important to specify that the screws ${}^4\$_1^5$ and ${}^5\$_1^6$ of the SP-type limb as well as the screw ${}^5\$_2^6$ of the SPR-type limb are auxiliary elements that are included in order to satisfy an algebraic requirement of the Lie algebra $e(3)$, naturally the joint rates of these fictitious kinematic pairs are null.

Forward velocity analysis (FVA): Given the active joint velocity rates ${}_3\omega_4^i$ of the robot, the FVA consists of finding the translational velocity of the control point Cm. To this end, consider that the screw ${}^1\$_i^2$ is reciprocal to all the screws representing revolute joints in the same limb due to the fact that the direction of ${}^1\$_i^2$ intersect at a common point the primal parts of those screws. Hence, the application of the Klein form $\{*;*\}$ of the Lie algebra $e(3)$ of ${}^1\$_i^2$ to both sides of the corresponding Eq. (19), the reduction of terms leads to

$$\left\{{}^1\$_i^2; \boldsymbol{V}_O\right\} = {}_3\omega_4^i. \tag{20}$$

Consider the SP limb. Since the primal parts of the screw ${}^0\$_1^1$ and ${}^2\$_1^3$ are perpendicular to the dual part of the screw ${}^3\$_1^4$ and in addition intersect the primal parts of the remaining screws simulating the spherical joint S_1, then considering that ${}_4\omega_5^1 = {}_5\omega_6^1 = 0$ the systematic application of the Klein form of ${}^0\$_1^1$ and ${}^2\$_1^3$ to both sides of the corresponding Eq. (19) with the cancellation of terms it follows that

$$\left\{{}^0\$_1^1; \boldsymbol{V}_O\right\} = \left\{{}^2\$_1^3; \boldsymbol{V}_O\right\} = 0. \tag{21}$$

The FVA is completed by resorting to the SPR limb. The primal part of the screw ${}^0\$_1^1$ exhibits the following characteristics: (i) it is parallel to the primal part of the screw ${}^4\$_1^5$, representing the revolute joint connecting the limb to the coupler platform; (ii) it is perpendicular to the dual part of the screw ${}^3\$_1^4$ associated to the prismatic joint; (iii) it intersects at a common point the primal parts of the screws ${}^1\$_1^2$ and ${}^2\$_1^3$. With these considerations in mind, the application of the Klein form of ${}^0\$_1^1$ to both sides of the corresponding Eq. (19) leads to

$$\left\{{}^0\$_2^1; \boldsymbol{V}_O\right\} = 0. \tag{22}$$

Casting into a matrix vector form Eqs. (20)–(22), it is possible to write

$$\mathbf{J}^T \, \Delta \boldsymbol{V}_O = \dot{\mathbf{q}}, \tag{23}$$

where $\mathbf{J} = [{}^1\$_1^2, {}^1\$_2^2, {}^1\$_3^2, {}^0\$_1^1, {}^2\$_1^3, {}^0\$_2^1]$ is the active Jacobian of the robot, $\dot{\mathbf{q}} = [{}_3\omega_4^1 \; {}_3\omega_4^2 \; {}_3\omega_4^3 \; 0 \; 0 \; 0]^{\mathrm{T}}$, and $\Delta = \begin{bmatrix} \boldsymbol{O}_{3\times3} & \mathbf{I}_3 \\ \mathbf{I}_3 & \boldsymbol{O}_{3\times3} \end{bmatrix}$ is an operator of polarity. Furthermore, once the velocity state $\boldsymbol{V}_O$ is computed by means of expression (23), the translational velocity of the control point Cm is obtained by applying the concept of helicoidal vector fields, see Gallardo-Alvarado *et al.*,[24] as follows:

$$\boldsymbol{v}_{Cm} = \mathcal{D}(\boldsymbol{V}_O) + \mathcal{P}(\boldsymbol{V}_O) \times \boldsymbol{r}_{Cm/O}. \tag{24}$$

Inverse velocity analysis (IVA): Given a prescribed velocity state $\boldsymbol{V}_O$, the IVA consists of finding the required joint velocity rates of the robot, or in other words the matrix Ω_i. This analysis is solved directly from expression (19)

$$\Omega_i = (\mathbf{J}_i)^{-1} \, \boldsymbol{V}_O. \tag{25}$$

4.2. Singularity analysis

A singularity occurs when the coupler platform gains or loses degrees of freedom. Usually is an undesirable characteristic of parallel manipulators that must be treated properly in order to avoid physical damages to it.

As an intermediate step, in what follows the mobility of each one of the limbs of the EPM is investigated as follows: (i) SP limb. This serial connecting chain allows the coupler platform to have an arbitrary displacement, provided by the prismatic pair, and an arbitrary orientation, provided by the spherical pair, with respect to the fixed platform. This set of possible displacements does not form a subgroup of the Euclidean group; however, the set has four degrees of freedom. Clearly, the two loss degrees of freedom of this kinematic chain are due to the fixed connection at the coupler platform. Moreover, since ${}^4\$_1^5$ and ${}^5\$_1^6$ are auxiliary screws, then these elements can be chosen in such a way that cannot be obtained as linear combinations of the reaming screws and are disregarded from the singularity analysis. Furthermore, the screws ${}^0\$_1^1$, ${}^1\$_1^2$, and ${}^2\$_1^3$ associated to the revolute joints representing the spherical joint are, evidently, linearly independent and cannot generate the screw ${}^3\$_1^4$ representing the prismatic pair. Therefore, the SP-type limb is free of singularities if the velocity state $\boldsymbol{V}_{B_1}$ is a four-dimensional vector where the dual part is a vector along the line S_1B_1. (ii) SPR limb. This serial connecting chain allows the coupler platform to have two arbitrary displacements due to the prismatic and revolute joints, and an arbitrary orientation, provided by the spherical joint, with respect to the fixed platform. This set has five degrees of freedom and does not form a subgroup of the Euclidean group. The screw ${}^5\$_2^6$ is a an auxiliary element and therefore does not affect the singularity analysis. Since the prismatic joint is perpendicular to the revolute joint, and the spherical pair does not lie along the axis of the revolute joint, the SPR limb is free of singularities if the velocity state $\boldsymbol{V}_{B_2}$ is a five-dimensional vector where the dual part is a vector in the plane formed by the lines S_2B_2 and a line perpendicular to the axis of the revolute joint. (iii) SPU limb. Since none of the axes of the two revolute joints that form the universal pair passes through the common point of the spherical pair and the direction of the prismatic pair does not coincide with the axes of the revolute pairs of the universal joint; the serial connecting chain generates all the possible displacements of the Euclidean group. Thus, if the coupler platform was connected to the fixed platform

https://doi.org/10.1017/S026357471100083X Published online by Cambridge University Press

only by the serial chain SPU, the moving platform could adopt any arbitrary pose, within the workspace of the serial connecting chain, with respect to the fixed platform.

On the other hand, it is well known that most singularities are related with the infinitesimal kinematics; however, as noted by Di Gregorio,[6] a global singularity emerges if some closure equations dealing with the finite kinematics are dependent, for the manipulator at hand such expressions are $(\boldsymbol{B}_i - \boldsymbol{S}_i) \bullet (\boldsymbol{B}_i - \boldsymbol{S}_i) - q_i^2 = 0$. In this type of singularity, the coupler platform can undergo finite displacements without changing the length of the asymmetrical limbs. The next type of singularities to be treated iss related with the infinitesimal kinematics of the robot. To this aim, expression (23) is rewritten as

$$\mathbf{A}\boldsymbol{V}_O = \mathbf{B}\dot{\mathbf{q}}, \tag{26}$$

where $\mathbf{A} = \mathbf{J}^{\mathrm{T}}\ \Delta$ and $\mathbf{B}$ is the identity matrix. In a singular configuration, the coupler platform cannot perform an arbitrary velocity state $\boldsymbol{V}_O$ with respect to the fixed platform. Before do any further in this way, it is prudent to disregard trivial situations like (i) if any of the length limbs q_i vanishes then the computation of some infinitesimal screws is indefinite; (ii) if the coupler platform is at rest, in other words $\boldsymbol{V}_O = [\boldsymbol{O} \quad \boldsymbol{O}]^{\mathrm{T}}$, then according to Eq. (23) one possibility that satisfies this velocity state is such that ${}_3\omega_4^1 = {}_3\omega_4^2 = {}_3\omega_4^3 = 0$; a similar conclusion emerges from expression (25). The other possibility is that $\det(\mathbf{J}) = 0$, which implies that the robot admits arbitrary values for ${}_3\omega_4^1$, ${}_3\omega_4^2$, and ${}_3\omega_4^3$; (iii) if $e = 0$ then the rotation matrix ${}^1\mathbf{R}^0$ is indefinite.

According to expression (26), a singular configuration emerges when (i) matrix $\mathbf{A}$ is singular, namely, singularity type 2; (ii) matrix $\mathbf{B}$ is singular, namely, singularity type 1; (iii) $\mathbf{A}$ and $\mathbf{B}$ are both singular, namely, singularity type 3. For details, the reader is referred to Gosselin and Angeles.[25]

Singularity type 2 is concerned with the forward kinematics of the robot. Clearly, matrix $\mathbf{A}$ is singular when the active Jacobian matrix $\mathbf{J}$ is singular. Hence, in order to approach the singularities dealing with the FVA of the parallel manipulator under study, the active Jacobian $\mathbf{J}$ is recalled here

$$\mathbf{J} = \left[{}^1\$_1^2,\ {}^1\$_2^2,\ {}^1\$_3^2,\ {}^0\$_1^1,\ {}^2\$_1^3,\ {}^0\$_2^1\right]. \tag{27}$$

The detection of this type of singularity can be achieved by analyzing the linear dependence of the elements, or reciprocal screws, of the matrix $\mathbf{J}$ as well to setting the determinant of $\mathbf{J}$ to zero. Considering that the reciprocal screws ${}^0\$_1^1$, ${}^2\$_1^3$, and ${}^0\$_2^1$ belong to the same plane then a brief inspection of Eq. (27) reveals that according to the concept of linear dependence, the robot is at singularity, among other circumstances, if the primal parts of the reciprocal screws ${}^1\$_1^2$, ${}^1\$_2^2$, and ${}^1\$_3^2$ are concurrent or belong to the same plane. A complete analysis can be obtained by considering $\det(\mathbf{J}) = 0$. However, it must be noted that the symbolic computation of this determinant is a hazardous task due to the generation of higher order polynomials, with radicals, in the unknowns q_i, the handling of such expression could be a tedious task. In order to overcome this drawback, the following algorithm is proposed:

$$\left.\begin{array}{l}\text{Define intervals for } q_1 \text{ and } q_2\\ \text{Compute the coordinates of } S_1,\\ \text{Compute the coordinates of } S_2,\\ \text{Compute the coordinates of } S_3,\\ \text{Compute the transformation matrix } {}^1\mathbf{T}^0,\\ \text{Compute } {}^0\mathbf{T}^1 = ({}^1\mathbf{T}^0)^{-1}\\ \text{Compute the coordinates of } B_i,\\ \text{Compute the reciprocal screws,}\\ \text{Compute the active Jacobian matrix } \mathbf{J},\\ \text{Compute } q_3 \text{ considering } det(\mathbf{J}) = 0,\\ \text{Save the singular point } (q_1, q_2, q_3).\end{array}\right\} \tag{28}$$

Once this procedure is completed, a singular surface can be generated from the computed points.

On the other hand, since matrix $\mathbf{B}$ is precisely the identity matrix then the robot is free of singularities type 1 and 3.

Finally, although the isotropic analysis is not included in this work, it is worth to note that the EPM is fully isotropic, concerning with the inverse kinematics, since $\det(\mathbf{B}) = 1$.

4.3. Acceleration analysis

The reduced acceleration state of the coupler platform with respect to the fixed platform taking the origin of the global reference frame as the reference pole, $\boldsymbol{A}_O = [\mathcal{P}(\boldsymbol{A}_O) = \dot{\boldsymbol{\omega}}, \mathcal{D}(\boldsymbol{A}_O) = \boldsymbol{a}_O - \boldsymbol{\omega} \times \boldsymbol{v}_O]^{\mathrm{T}}$, can be written through any of the limbs of the EPM as follows:

$$\mathbf{J}_i\dot{\Omega}_i + \mathcal{L}_i = \boldsymbol{A}_O, \tag{29}$$

where $\dot{\Omega}_i = [{}_0\dot{\omega}_1^i,\ {}_1\dot{\omega}_2^i,\ {}_2\dot{\omega}_3^i,\ {}_3\dot{\omega}_4^i,\ {}_4\dot{\omega}_5^i,\ {}_5\dot{\omega}_6^i]^{\mathrm{T}}$ is a matrix containing the joint acceleration rates of the ith limb and

$$\mathcal{L}_i = \sum_{j=0}^{4}\left[{}_j\omega_{j+1}^i\,{}^j\$_i^{j+1} \qquad \sum_{k=j+1}^{5}{}_k\omega_{k+1}^i\,{}^k\$_i^{k+1}\right] \tag{30}$$

is the Lie screw of acceleration in which the brackets $[*\quad *]$ denote the Lie product of the Lie algebra $e(3)$.

Forward acceleration analysis (FAA): Given the active joint acceleration rates ${}_3\dot{\omega}_4^i$ of the robot, the FAA consists of finding the translational acceleration of the control point Cm.

The application of the Klein form of each one of the reciprocal screws with both sides of Eq. (29) and casting into a matrix-vector form, a compact acceleration equation is obtained as follows:

$$\mathbf{J}^{\mathrm{T}}\ \Delta\boldsymbol{A}_O = \begin{bmatrix}{}_3\dot{\omega}_4^1 + \{{}^1\$_1^2; \mathcal{L}_1\}\\ {}_3\dot{\omega}_4^2 + \{{}^1\$_2^2; \mathcal{L}_2\}\\ {}_3\dot{\omega}_4^3 + \{{}^1\$_3^2; \mathcal{L}_3\}\\ \{{}^0\$_1^1; \mathcal{L}_1\}\\ \{{}^2\$_1^3; \mathcal{L}_1\}\\ \{{}^0\$_2^1; \mathcal{L}_2\}\end{bmatrix}. \tag{31}$$

Furthermore, once the reduced acceleration state $\boldsymbol{A}_O$ is computed by means of expression (31), the translational

https://doi.org/10.1017/S026357471100083X Published online by Cambridge University Press

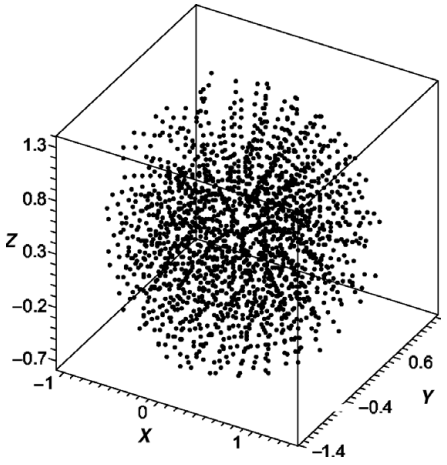

Fig. 2. Workspace of the numerical example.

acceleration of the control point Cm is obtained by applying the concept of helicoidal vector fields, for details see Gallardo-Alvarado *et al.*,[24] as follows:

$$\boldsymbol{a}_{Cm} = \mathcal{D}(\boldsymbol{A}_O) + \mathcal{P}(\boldsymbol{A}_O) \times \boldsymbol{r}_{Cm/O} + \boldsymbol{\omega} \times \boldsymbol{v}_{Cm}. \tag{32}$$

Inverse acceleration analysis (IAA): Given a prescribed reduced acceleration state $\boldsymbol{A}_O$, the IAA consists of finding the required joint acceleration rates of the robot, or in other words, the matrix $\dot{\Omega}_i$. This analysis is solved directly from expression (29)

$$\dot{\Omega}_i = (\mathbf{J}_i)^{-1}(\boldsymbol{A}_O - \mathcal{L}_i). \tag{33}$$

5. Numerical Results and Discussion

In this section, a numerical example is provided. The unit vector along the axis of the revolute joint of the SPR limb, expressed in the moving reference frame o_xyz, is given by $\hat{u} = .866\hat{i} + 0.5\hat{k}$ whereas, using hereafter SI units, the coordinates of points S_i, expressed in the fixed reference frame O_XYZ, are chosen as $S_1 = (0, 0, 0)$, $S_2 = (0, 0, 0.5)$, and $S_3 = (0.433, 0, 0.25)$. Furthermore, the side of the equilateral triangle $\Delta B_1 B_2 B_3$ is given by $e = B_{12} = B_{23} = B_{13} = 0.5$.

In order to estimate the workspace, consider the interval $0.5 \leq q_i \leq 1.5$ for each generalized coordinate q_i. After, including reflected solutions, 1914 real points are computed for the center of the end-effector platform, also called the control point, see Fig. 2.

Furthermore, the direct singular surfaces, using the algorithm reported in Section 4.2, are presented in Fig. 3. The combinations of the signs of the discriminants are placed at the top of each plot. It is important to mention that singular surfaces provided by combinations with distinct signs, $+1 - 1$ and $-1 + 1$, are associated to spurious solutions of the FDA. Thus, the only feasible direct singular configurations are the provided by the combinations $+1 + 1$ and $-1 - 1$.

In what follows, the simulations are to command the control point Cm of the end-effector platform to move according to the periodical function $Cm = (0.14433 + 0.25\sin(t), 1 - 0.25\sin(t)\cos(t), 0.25 - 0.25\sin^2(t))$ where the interval for the time t is given by $0 \leq t \leq 2\pi$. The resulting time history of the required active length limbs q_i to satisfy such function is provided in Fig. 4.

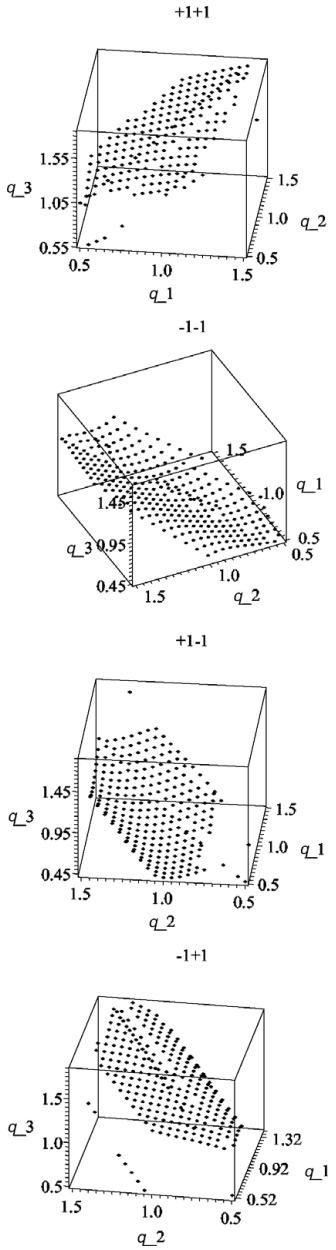

Fig. 3. The direct singular surface.

Finally, consider the generalized coordinates $q_1 = 1.0 - 0.1\sin^2(t)$, $q_2 = 1.0 - 0.15\sin(t)\cos(t)$, and $q_3 = 1.0 - 0.125\sin^3(t)$, then the time history of the translational acceleration of the end-effector platform is provided in Fig. 5, together with the numerical results generated using the software ADAMS©. Please note that the numerical results obtained by using screw theory are in excellent agreement with those generated with ADAMS©.

6. Conclusions

In this work, a novel translational manipulator is introduced. The proposed robot is formed with an asymmetrical active parallel manipulator with SP + SPR + SPU type limbs and

https://doi.org/10.1017/S026357471100083X Published online by Cambridge University Press

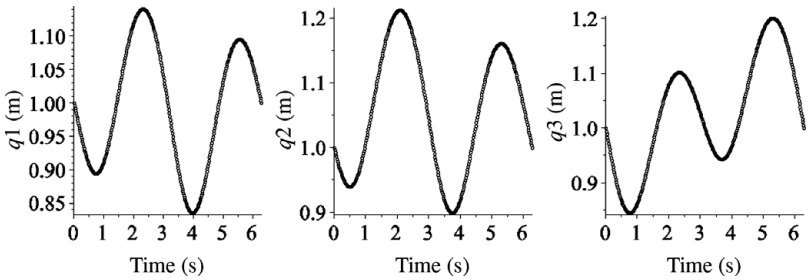

Fig. 4. Time history of the inverse position analysis.

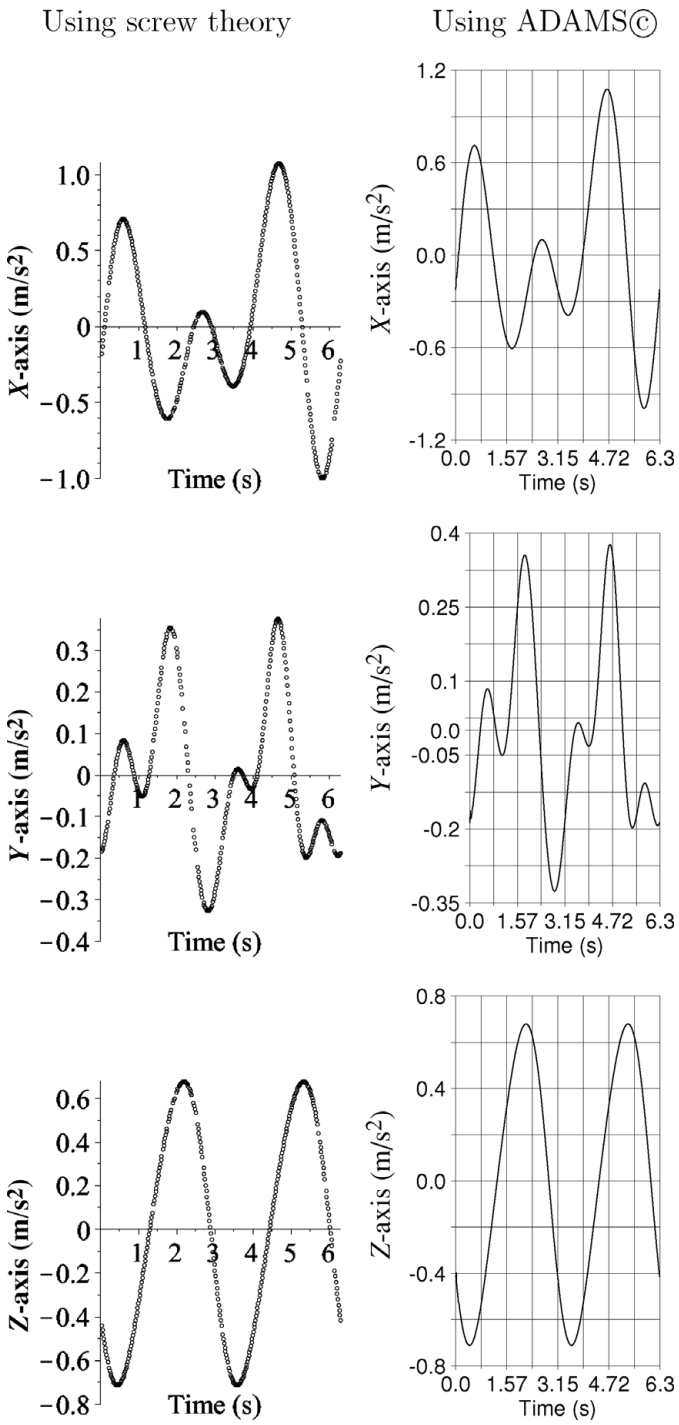

Fig. 5. Time history of the linear acceleration of point C_m.

a well-known symmetrical TPM. The main benefits of the topology of the proposed robot are (i) an exact solution is available to solve the FDA; (ii) the actual configuration of the robot can be determined choosing the signs of discriminants associated to two simple second-order algebraic equations; (iii) unlike other reported works, see for instance,[8,26] the FDA does not require the application, among other methods, of the Sylvester dialytic elimination method because the obtained nonlinear equations are solved sequentially and not simultaneously; iv) the degrees of freedom between the coupler and fixed platform are partially decoupled.

The infinitesimal kinematics of the robot is approached by means of the theory of screws. Simple and compact expressions for solving the forward infinitesimal kinematics are easily derived by taking advantage of the concept of reciprocal screws. It is worth to mention that with this procedure the FAA does not require the computation of the passive joint acceleration rates of the manipulator. Applications of the proposed robot include any task of a TPM, such as simple pick-and-place operations, assembling, and welding. Furthermore, although this work does not approach the kinetic analysis, it is straightforward to demonstrate that, due to linear actuators instead of revolute actuators, the proposed robot can be used as a multiaxis machine tool. Finally, a numerical example is provided. This example includes the computation of the workspace, based on the FDA, as well as the computation of the direct singular surfaces of the robot and the application of the inverse displacement analysis. The example finishes with the application of the forward infinitesimal kinematics of the end-effector platform. Furthermore, the numerical results dealing with the acceleration analysis are successfully compared with numerical results generated with a commercially available software of kinematics simulation like ADAMS©.

Acknowledgment

This work was supported by National Council of Science and Technology, Conacyt, of México.

Appendix. Coefficients *K*

Let $B_i = (bx_i, 0, bz_i)$, $u = (u_x, 0, u_z)$ then the coefficients of expressions (4), (5), (7), and (8) are given by

$$K_1 = u_z q_1/(-u_x bz_1 + u_x bz_2 + bx_1 u_z - bx_2 u_z),$$

https://doi.org/10.1017/S026357471100083X Published online by Cambridge University Press

$$K_2 = (-2u_x bx_2 bz_1 + 2u_x bx_2 bz_2 - bx_2^2 u_z - 2u_z bz_2 bz_1 + u_z bz_2^2 + u_z bx_1^2 + u_z q_2^2 + u_z q_1^2 + u_z bz_1^2 - u_z e^2) /2(-u_x bz_1 + u_x bz_2 + bx_1 u_z - bx_2 u_z),$$

$$K_6 = -u_x q_1/(-u_x bz_1 + u_x bz_2 + bx_1 u_z - bx_2 u_z),$$

$$K_7 = (u_x bx_1^2 - u_x e^2 + u_x q_1^2 - 2bx_1 u_z bz_2 + u_x bz_1^2 - 2bx_1 u_x bx_2 + u_x bx_2^2 - u_x bz_2^2 + u_x q_2^2 + 2bx_2 u_z bz_2) /2(u_x bz_1 - u_x bz_2 - bx_1 u_z + bx_2 u_z),$$

$$K_3 = K_1^2 + K_6^2 + 1,$$

$$K_4 = 2q_1 + 2(K_2 - bx_1)K_1 + 2(K_7 - bz_1)K_6,$$

$$K_5 = (K_2 - bx_1)^2 - e^2 + (K_7 - bz_1)^2 + q_1^2,$$

$$K_8 = (2bz_3 Y_2 - 2Z_2 q_1 - 2Y_2 bz_1 + 2bz_3 q_1) /2(-bx_1 Z_2 + bx_3 Z_2 + X_2 bz_1 - bx_3 bz_1 - X_2 bz_3 + bx_1 bz_3),$$

$$K_9 = (bx_3^2 bz_1 - bx_3^2 Z_2 + bz_3 X_2^2 - X_2^2 bz_1 - bz_3 q_1^2 + Z_2 bx_1^2 - Y_2^2 bz_1 - Z_2^2 bz_1 + e^2 bz_1 - bz_3 bx_1^2 + bz_3^2 bz_1 + Z_2 bz_1^2 - bz_3^2 Z_2 - q_3^2 bz_1 - e^2 Z_2 + q_3^2 Z_2 + bz_3 Y_2^2 + bz_3 Z_2^2 - bz_3 bz_1^2 + Z_2 q_1^2) /2(bx_1 Z_2 - bx_3 Z_2 - X_2 bz_1 + bx_3 bz_1 + X_2 bz_3 - bx_1 bz_3),$$

$$K_{13} = (X_2 q_1 - bx_3 Y_2 - bx_3 q_1 + bx_1 Y_2) /(-bx_1 Z_2 + bx_3 Z_2 + X_2 bz_1 - bx_3 bz_1 - X_2 bz_3 + bx_1 bz_3),$$

$$K_{14} = (-bx_3 bx_1^2 + X_2 bz_1^2 - bx_1 X_2^2 + X_2 q_1^2 - X_2 bx_3^2 - X_2 bz_3^2 + X_2 q_3^2 - X_2 e^2 + bx_3 Z_2^2 + bx_3 Y_2^2 + bx_3 X_2^2 - bx_3 bz_1^2 - bx_3 q_1^2 + bx_1 bx_3^2 + bx_1 bz_3^2 - bx_1 q_3^2 + bx_1 e^2 - bx_1 Z_2^2 - bx_1 Y_2^2 + X_2 bx_1^2) /2(-bx_1 Z_2 + bx_3 Z_2 + X_2 bz_1 - bx_3 bz_1 - X_2 bz_3 + bx_1 bz_3),$$

$$K_{10} = K_8^2 + K_{13}^2 + 1,$$

$$K_{11} = 2q_1 + 2(K_9 - bx_1)K_8 + 2(K_{14} - bz_1)K_{13},$$

$$K_{12} = (K_9 - bx_1)^2 - e^2 + (K_{14} - bz_1)^2 + q_1^2.$$

References

1. Available in the website http:parallelmic.org.
2. R. Clavel, "DELTA: A Fast Robot with Parallel Geometry," *Proceedings of the 18th International Symposium on Industrial Robots*, Sydney (1988) pp. 91–100.
3. L. W. Tsai, "Kinematics of a Three-DOF Platform Manipulator with Three Extensible Limbs," **In**: *Advances in Robot Kinematics* (J. Lenarcic and V. Parenti-Castelli, eds.) (Kluwer Academic Publishers, London, 1996) pp. 401–410.
4. P. Wenger and D. Chablat, "Kinematic Analysis of a New Parallel Machine Tool: The Orthoglide," **In**: *Advances in Robot Kinematics* (J. Lenarčič and M. L. Stanisič, eds.) (Kluwer Academic Publishers, London, 2000) pp. 305–314.
5. T. S. Zhao and Z. Huang, "A Novel Three-DOF Translational Platform Mechanism and Its Kinematics," *Proceedings of the 2000 ASME Design Engineering Technical Conferences*, Baltimore (2000) paper DETC2000/MECH–14101.
6. R. Di Gregorio, "Kinematics of the Translational 3-URC Mechanism," *Proceedings of the IEEE/ASME International Conference on Advanced Intelligent Mechatronics*, Como (2001) pp. 147–152.
7. X. Kong and C. M. Gosselin, "Kinematics and singularity analysis of a novel type of 3-CRR 3-DOF translational parallel manipulator," *Int. J. Robot. Res.* **21**(9), 791–798 (2002).
8. M. Callegari and M. Tarantini, "Kinematic analysis of a novel translational platform," *ASME J. Mech. Des.* **125**(2), 308–315 (2003).
9. G. Gogu, "Structural synthesis of fully-isotropic translational parallel robots via theory of linear transformations," *Eur. J. Mech. A/Solids* **23**(6), 1021–1039 (2004).
10. G. Gogu, "Mobility Criterion and Overconstraints of Parallel Manipulators," *Proceedings of the CK2005, International Workshop on Computational Kinematics,* Cassino (2005) p. 22.
11. Y. Li and Q. Xu, "Kinematics and Dexterity Analysis for a Novel 3-DOF Translational Parallel Manipulator," *Proceedings of the 2005 IEEE International Conference on Robotics and Automation*, Barcelona (2005) pp. 2955–2960.
12. W. Li, F. Gao and J. Zhang, "R-CUBE, a decoupled parallel manipulator only with revolute joints," *Mech. Mach. Theory* **40**(4), 467–473 (2005).
13. M. Callegari, M. Palpacelli and M. Scarponi, "Kinematics of the 3-CPU Parallel Manipulator Assembled for Motions of Pure Translation," *Proceedings of the 2005 IEEE International Conference on Robotics and Automation*, Barcelona (2005) pp. 4031–4036.
14. M. Callegari, M. C. Palpacelli and M. Principi, "Dynamics modelling and control of the 3-RCC translational platform," *Mechatronics* **16**, 589–605 (2006).
15. M. Ruggiu, "Kinematics analysis of the CUR translational manipulator," *Mech. Mach. Theory* **43**(9), 1087–1098 (2008).
16. X. Kong and C. M. Gosselin, "Type Synthesis of Linear Translational Parallel Manipulators," **In**: *Advances in Robot Kinematics—Theory and Applications* (J. Lenarčič and F. Thomas, eds.) (Kluwer Academic Publishers, 2002) pp. 411–420.
17. X. Kong and C. M. Gosselin, "Type synthesis of 3-DOF translational parallel manipulators based on screw theory," *ASME J. Mech. Des.* **126**(1), 83–92 (2004).
18. M. Carricato and V. Parenti-Castelli, "Singularity-free fully-isotropic translational parallel mechanisms," *Int. J. Robot. Res.* **21**(2), 161–174 (2002).
19. S. Briot and I. A. Bonev, "Pantopteron: A new fully decoupled 3DOF translational parallel robot for pick-and-place applications," *ASME J. Mech Robotics* **1**(1), 021001 (2009).
20. M. G. Her, C. Y. Chen, M. Karkoub and Y. C. Hung, "A generalised approach to point-to-point motion of multi-DOF parallel manipulators illustrated with TMPM," *Int. J. Adv. Manuf. Technol.* **22**, 216–223 (2003).
21. J. Gallardo-Alvarado, J. M. Rico-Martínez and G. Alici, "Kinematics and singularity analyses of a 4-DOF parallel manipulator using screw theory," *Mech. Mach. Theory* **41**, 1048–1061 (2006).
22. J. Gallardo-Alvarado, C. R. Aguilar–Nájera, L. Casique-Rosas, L. Pérez-González and J. M. Rico-Martínez, "Solving the kinematics and dynamics of a modular spatial hyper-redundant manipulator by means of screw theory," *Multibody Syst. Dyn.* **20**, 307–325 (2008).

https://doi.org/10.1017/S026357471100083X Published online by Cambridge University Press

23. L.-W. Tsai, *Robot analysis* (John Wiley & Sons, New York, 1999).
24. J. Gallardo-Alvarado, H. Orozco-Mendoza and R. Rodríguez-Castro, "Finding the jerk properties of multibody systems using helicoidal vector fields," *Inst. Mech. Engr. Part C: J. Mech. Eng. Sci.* **222**(11), 2217–2229 (2008).
25. C. Gosselin and J. Angeles, "Singularity analysis of closed-loop kinematic chains," *IEEE Trans. Robot. Autom.* **6**(3), 261–290 (1990).
26. B. Roth, "Computation in Kinematics," **In**: *Computational Kinematics* (J. Angeles, G. Hommel and P. Kovacs, eds.) (Kluwer Academic Publishers, Dordrecht, The Netherlands, 1993) pp. 314.

https://doi.org/10.1017/S026357471100083X Published online by Cambridge University Press